31st EPS Conference on Plasma Phys. London, 28 June - 2 July 2004 ECA Vol.**28G**, P-4.187 (2004)

Transport in the presence of ITBs in the MAST Spherical Tokamak

A. R. Field, R. J. Akers, C. Brickley, P. G. Carolan, C. Challis, N. J. Conway,

G. Cunningham, H. Meyer, C. Roach, M. J. Walsh[1] and the MAST team

EURATOM/UKAEA Fusion Association, Culham Science Centre, Abingdon, Oxon, OX14 3DB, UK
(1) Walsh Scientific Ltd., Culham Science Centre, Abingdon, Oxon, OX14 3EB, UK

Introduction

The physics of Internal Transport Barriers (ITBs) is an active area of research [1], with ITBs utilised in advanced tokamak scenarios, both to optimise confinement and the bootstrap contribution to the non-inductive current drive. ITBs are formed when anomalous transport is suppressed to about the ion neo-classical level through decorrelation of micro-turbulence by strong E×B flow shear [2] in the presence of weak magnetic shear, s, which reduces instability growth rates [3]. The spherical tokamak (ST) provides a unique environment for studies of ITB formation in high-β, low aspect ratio plasmas, where it is predicted that ITG turbulence may be suppressed by the intrinsic pressure driven flow shear alone, with the ratio of the E×B shearing rate, ω_{SE}, to the instability growth rate, γ_m, predicted to scale as $\omega_{SE}/\gamma_m \sim \rho_i *$ [4].

In MAST, ITBs have been produced by NBI heating (~ 2 MW) of low-density discharges during a current ramp to produce weak/reversed magnetic shear and high toroidal rotation (~ 250 km/s) [5]. Marked differences in the ITB character between similar discharges with co- and counter-NBI heating highlight the profound influence that changes to the E×B shearing rate and the magnetic shear can have on anomalous transport [6, 7]. Profile data from these discharges have been submitted to the ITPA profile database, which has been used for multi-machine studies both of ITB formation and evolution [8] and of ITB existence criteria [9]. Here the transport in these discharges is discussed in more detail and some general comments are presented on ITB existence criteria that are appropriate under conditions of high driven toroidal flow.

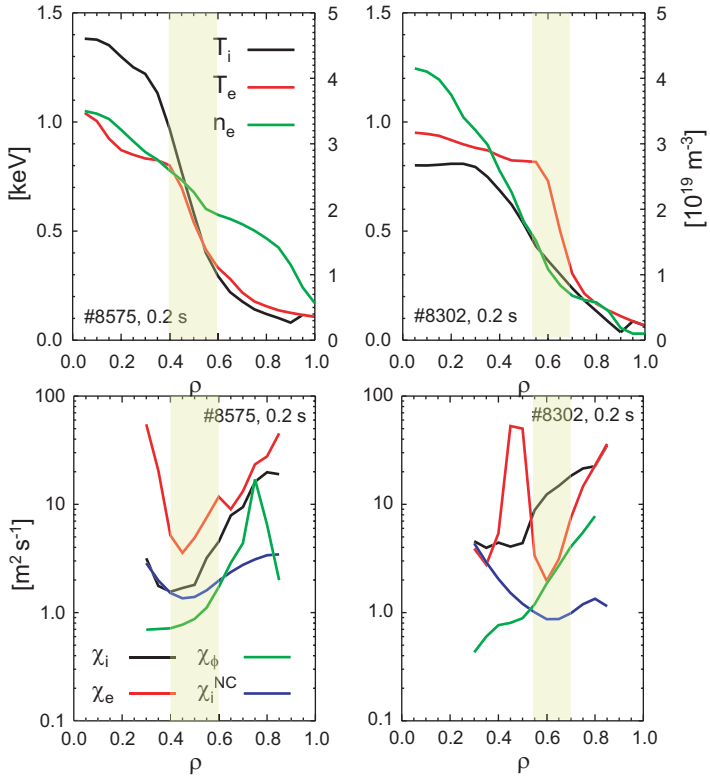

Fig. 1 (a) Profiles of T_e, T_i and n_e vs normalised radius ρ during ITB discharges with co- (#8575) and counter- (#8302) NBI heating at 0.2 s and (b) the corresponding thermal, χ_i, χ_e, and momentum, χ_ϕ, diffusivities from TRANSP analysis. The neo-classical ion χ_i^{NC} (Z-corrected Chang-Hinton) is shown for comparison.

Transport Analysis

Transport analysis of ITB discharges using TRANSP is based upon high-quality measurements of kinetic profiles from TS (T_e, n_e) and CXRS (T_i, $V_{i\phi}$) and Z_{eff} and neutral sources from imaging profile diagnostics

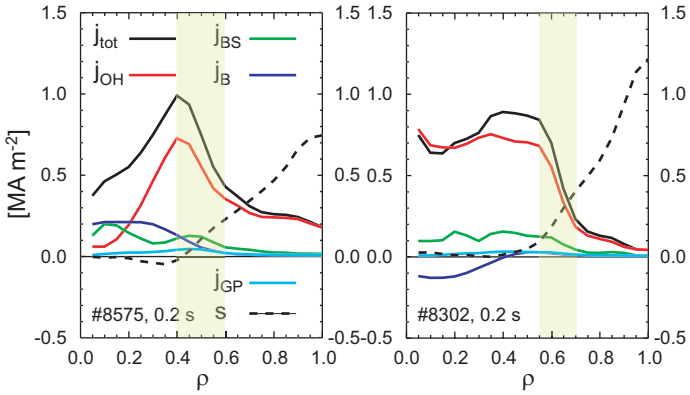

Fig. 2 Profiles of total current density, j_{tot}, and magnetic shear, s, from TRANSP analysis of discharges in Fig. 1. Bootstrap, j_{BS}, Ohmic, j_{OH}, pressure, j_{GP}, and NBI driven, j_B, contributions are shown.

[6]. A comparison of $T_{i,e}$ and n_e profiles from comparable ITB discharges with co- and counter-NBI heating is shown in Fig. 1 together with the associated thermal, $\chi_{i,e}$, and momentum, χ_ϕ, transport coefficients. The neo-classical ion thermal diffusivity χ_i^{NC} (Z-corrected Chang-Hinton [10]) is also shown for comparison.

With co-NBI an ion ITB is produced with $\chi_i \sim \chi_i^{NC}$ at $\rho = r/a \sim 0.5$, which corresponds to the location where $s = (r/q)\,dq/dr \sim 0$ as shown in Fig. 2. There is a weaker suppression of the electron transport with $\chi_e \sim 2$–$3\ \chi_i$. The hollow current density profile results primarily from an off-axis peaking of the Ohmic current density. There is significant on axis NBCD and bootstrap contribution to the total current density. As shown in Fig. 3, the radial E-field, $E_r = \nabla p_i / eZ_i n_i + V_{i\phi} B_\theta - V_{i\theta} B_\phi$, is predominantly due to the driven toroidal flow, $V_{i\phi}$, with the pressure gradient contribution reducing the net positive plasma potential. In Fig. 4 the corresponding ExB flow shear, $\omega_{SE} \cong \left| RB_\theta / B_\phi \, \partial(E_r / RB_\theta)/\partial r \right|$ is shown [11] which exhibits a maximum $\omega_{SE} \sim 6\times10^5$ s^{-1} at the ITB foot. This is compared with a prediction for the ITG growth rate, γ_m, as discussed further below.

With counter-NBI the dominant $V_\phi B_\theta$ contribution to E_r from toroidal flow results in a negative plasma potential and is augmented by the pressure gradient, resulting in higher values of $\omega_{SE} \sim 10^6$ s^{-1} at greater radius, $\rho \sim 0.6$. Under these conditions a broad electron ITB with steep ∇T_e is produced, with $\chi_e \sim 2\ \chi_i^{NC}$ at $\rho \sim 0.7$. The on-axis, counter-NBCD also helps broaden the low-s region compared to the co-NBI case. Remarkably, at the location of the eITB the ion thermal transport is high with $\chi_i \sim 10\ \chi_i^{NC}$.

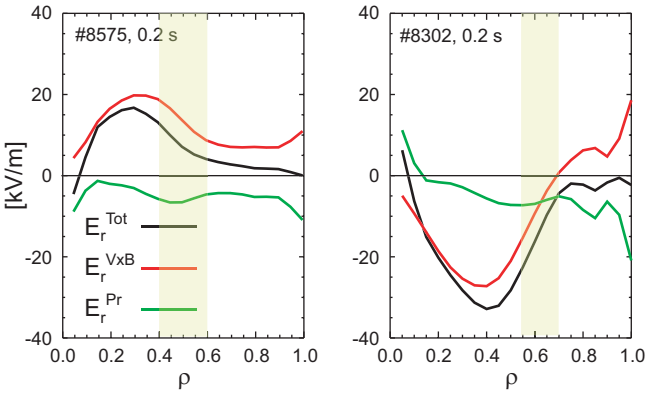

Fig. 3 Profiles of radial E-field, E_r, from TRANSP analysis of the discharges of Fig. 1 with contributions from the ExB flow, E_r^{VxB}, and pressure gradient, E_r^{Pr}, also shown.

Shear-flow stabilisation

Suppression of the anomalous transport should occur when the decorrelation due to the E×B shear exceeds the growth rate of the most unstable mode, $\omega_{SE} > \gamma_m$. An appropriate estimate of the ITG mode growth rate for conditions with low magnetic shear, $|L_n / L_s| >> 1$, where there is negligible overlap between modes on neighbouring resonant surfaces (where $m - nq = 0$) is $\gamma_m^{ITG} = (\eta_i - 2/3)^{3/4}\ |s|^{1/2}\ c_i / |L_s|$ where $\eta_i = L_n / L_T$, $c_i = (T_i / m_i)^{1/2}$

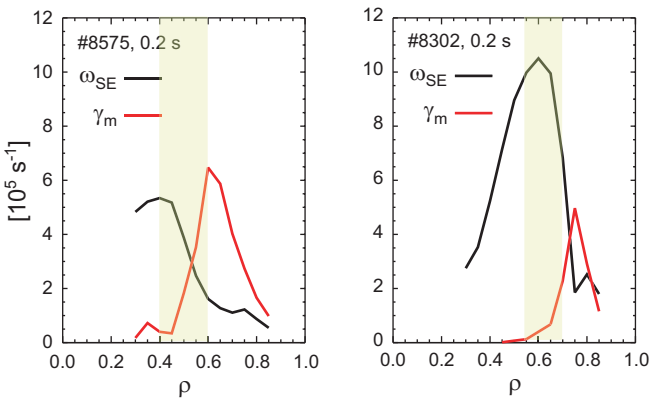

Fig. 4 Comparison of the E×B shearing rate, ω_{SE}, with the maximum predicted ITG growth rate, γ_m, for the discharges shown in Fig. 1.

and $L_s = qR/s$ [12]. This form for γ_m^{ITG} is appropriate for conditions where toroidicity enhances the role of the parallel ion dynamics and resonant wave-particle interactions. This is different from that used in a similar study on JET of ITB discharges [13], in which an alternative form for γ_m^{ITG} is used, appropriate for conditions where toroidal effects can be neglected. In the co-NBI case shown in Fig. 4, $\omega_{SE} > \gamma_m^{ITG}$ in the vicinity of the ion ITB, consistent with the suppression of transport due to ITG turbulence in this region, where the criterion $|L_n / L_s| >> 1$ is also satisfied.

Although the E×B shearing rate is higher in the counter-NBI discharge, with $\omega_{SE} >> \gamma_m^{ITG}$ in the vicinity of the eITB, the ion transport in this region is high, while the electron transport is strongly reduced instead.

Existence criteria

MAST data have contributed to a multi-machine analysis of ITB existence criteria [9], where it was found that critera such as those on R/L_T or ρ_T*, where $\rho_T* = \rho_s / L_T$ and ρ_s is the ion Larmor radius at the sound speed, are not generally applicable. The criterion $\rho_T* > \rho_{ITB}* \sim 0.014$, was found to be a reliable indication of ITB existence over a wide variety of JET discharges [14]. It is justified from scaling arguments using a generic form for the growth rate of drift instabilities, $\gamma_m = (c_s/L_T)\, G_1(s, \beta, L_T, \tau_e, \nu*, \ldots)$ where G_1 is a function of order unity [15], and by assuming that the temperature gradient provides the dominant contribution to the ExB flow shear, resulting in the scaling $\omega_{SE} \sim (c_s/L_T)\, \rho_T*$. Under conditions prevailing on MAST with strong unbalanced tangential NBI heating, where the toroidal deuteron Mach number $M_\phi \sim 0.8$, the driven toroidal flow dominates the ExB flow shear and this criterion is not appropriate. Indeed, it is found that $\rho_T* / \rho_{ITB}* \sim 10$ even in non-ITB, MAST L-mode discharges. An alternative criterion can be similarly derived under the assumption that the torioidal flow dominates the ExB flow shear. This results in the scaling $\omega_{SE} \sim c_s/L_T$ suggesting that a critical toroidal Mach number $M_\phi > M_\phi^{ITB}(s, \beta, L_T, \tau_e, \nu*, \ldots)$ is required for ITB formation. Further experiments on MAST with improved CXRS mesurements of T_i and $V_{i\phi}$ are planned to study ITB onset conditions.

Discussion

Growth rates of micro-instabilities thought to cause anomalous transport are predicted to be lower in the presence of weak magnetic shear, $|s| \sim 0$, and a steep pressure gradient, β', both reducing the drive due to curvature and ∇B-drifts, respectively [16]. Micro-stability calculations for NSTX-like ST equilibria made using the GS2 code [17] show that growth rates for ITG ($k_\perp \rho_i \sim 0.4$) and ETG ($k_\perp \rho_e \sim 0.3$) modes, although initially increasing with β', are reduced when $\beta' = d\beta'/d\rho > 2$. Growth rates are also reduced by low magnetic shear,

with γ_m reduced by a factor ~ 2 when s is decreased from 1.3 to 0.3. In the MAST discharges discussed here, the prevailing values of $\beta' \sim 0.3–0.5$ are, however, well below the threshold predicted for the onset of β' stabilisation. It should be noted that flux-tube codes such as GS2 are unsuited to simulation of conditions where $|s| \sim 0$, where the radial separation of mode rational surfaces, $\Delta_{mrs} = 1/nq'$, can exceed the gradient scale lengths.

Recent analytic studies of micro-stability in the presence of a minimum in q shows that low magnetic shear can have a profound effect on the mode structure of trapped electron (TEM) and ITG modes [18], where radially extended modes are replaced by narrow modes at the resonant surfaces which would be less effective in generating transport. Critical values for the magnetic shear, s_{crit}, for the stabilisation of long wavelength drift modes ($(nq\rho_s/r)^2 < 1$) are given as $s_{crit} < \varepsilon_n$ ($= L_n/R$) for TEM modes and $s_{crit} < \varepsilon_T^{1/3}$ for ITG modes. A further prediction is that collisions may fully stabilise TEM modes in the presence of a steep density barrier where $\varepsilon_n << 1$. In both discharges in Fig. 1, the high-resolution TS measurements exhibit a local steepening of the density profile in the vicinity of the ITB at the LFS, which would favour TEM stability.

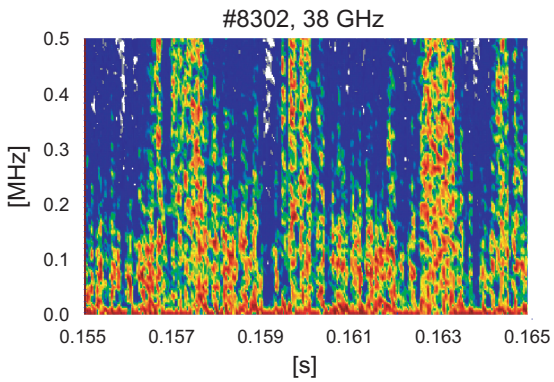

Fig. 5 Spectrogram of 38 GHz reflectometer signal from counter-NBI ITB discharge #8302.

A clue to the origin of the electron ITB in the counter-NBI discharge (#8302) is the observation of reduced density turbulence in the vicinity of the ITB observed by means of microwave reflectometry. The reflectometer signal, produced by velocity fluctuations at the cut-off layer ($n_e \sim 1.8\times10^{19}$ m^{-3}), exhibits periods during which the level of high frequency (0.2–0.5 MHz) turbulence is reduced by a factor ~ 2–3 compared to that in the co-NBI discharge (#8575), interupted by bursts of turbulence and MHD activity.

ITBs can be produced in MAST under conditions of high ExB flow shear and low magnetic shear where anomalous thermal transport is reduced to the ion neo-classical level. Formation of an electron ITB with counter-NBI may be due to the enhanced ExB shear and improved micro-stability at low magnetic shear, particularly in the presence of a steep density gradient.

References

[1] R. C. Wolf, Plasma Phys. Contr. Fus., **45** (2003) R1-R91.
[2] T. S. Hahm, K. H. Burrell, Phys. Plasmas, **2** 5 (1995) 1648-1651.
[3] T. S. Hahm, Plasma Phys. Contr. Fus., **44** (2002) A87-A101.
[4] M. Kotchenreuther, W. Dorland, Q. P. Liu et al., Nucl. Fusion, **40** 3Y (2000) 677.
[5] A.R.Field, R.J. Akers, N.J. Conway et al., 30th EPS, St. Petersburg, 2003, P3-93.
[6] R. J. Akers, J.W. Ahn, G.Y. Antar, et al., Plasma Phys. Contr. Fus, **45** (2003) A175-204.
[7] H. Meyer, PPCF, Plasma Phys. Contr. Fus., **46** 5A (2004) A291-A298.
[8] P. Gohil, J. Kinsey, V. Parail et al., Nucl. Fusion, **43** 8 (2003) 708-715.
[9] T. Fujita, T. Aniel, E. Barbato et al., 30th EPS, St Petersburg, 2003, P-2.13.
[10] C. S. Chang, F. L. Hinton, **29** (1986) 3314.
[11] R.V. Budny, B. Alper, D. N. Borba et al., Nucl. Fusion **42** (2002) 66-75.
[12] B. Esposito, F. Crisanti, V. Parail, 29th EPS, Montreux, 2002, O-1.07.
[13] A.L. Rogister, Nucl. Fusion, **41** 8 (2001) 1101-1106.
[14] G. Tresset, X. Litaudon, D. Moreau, X. Garbet, Nucl. Fusion, **42** (2002) 520-526.
[15] J. W. Connor, J. B. Taylor, Proc. 10th IAEA London, 1984, Vol. II (IAEA Vienna) p. 13.
[16] C. Bourdelle, Phys. Plasmas, **10** 7 (2003) 2881-2887.
[17] M. Kotchenreuther, G. Rewoldt, W. M. Tang, Comput. Phys. Commun., **88** (1995) 128.
[18] J. W. Connor, R. J. Hastie, 30th EPS, St. Petersburg, 2003, P3-94.

This work was funded jointly by the United Kingdom Engineering and Physical Sciences Research Council and by EURATOM.